URSI GASS 2021, Rome, Italy, 28 August – 4 September 2021

Wideband Interference Mitigation for SAR Based on Intrinsic Chirp Component Decomposition

Wenchang Han, Shiguo Mei, Weiwei Fan, Tian Tian, and Feng Zhou*
Key Laboratory of Electronic Information Countermeasure and Simulation Technology, Ministry of Education,
Xidian University, 710071 Xi'an, China

Abstract

The wideband interferences (WBIs) seriously degrade the quality of the synthetic aperture radar (SAR) image. Since the WBI occupies a larger bandwidth, it is difficult to mitigate it. Some existing WBI mitigation methods based on transform-domain analysis or filter design suffer from model mismatch and signal loss. In order to solve this problem, a method based on instantaneous frequency (IF) estimation and intrinsic chirp component decomposition (ICCD) is proposed to suppress WBI in this paper. First, a WBI-contaminated SAR echo is represented in the time-frequency domain by using the short-time Fourier transform (STFT). Then, the IF estimation is carried out for the WBI components. Finally, the WBI is extracted by using the ICCD. The experimental results verify the effectiveness of the proposed method.

1 Introduction

In recent decades, synthetic aperture radar (SAR) is widely applied in many civil and military fields [1, 2]. As the electromagnetic environment is becoming more and more complex, SAR echoes are unavoidable to be contaminated by wideband interferences (WBIs). The WBIs severely affect the imaging quality of the SAR system. With the WBI-corrupted SAR data, the estimation of Doppler parameters would be inaccurate, leading to a defocused image [3]. Besides, WBIs will cause some artifacts in the SAR image, making it difficult to carry out the image interpretation. Therefore, it is necessary to develop an effective approach for interference suppression to obtain well-focused SAR images and support the further research.

In recent years, a variety of methods were proposed to mitigate the WBI. Some methods are non-parametric, such as the instantaneous-spectrum notch filter and subspace projection. The SAR echo is transformed into the time-frequency domain by using the short-time Fourier transform (STFT), and the notch filtering or the eigensubspace projection (ESP) can be carried out for the instantaneous-spectrum [3]. A WBI mitigation method based on time-frequency transform and wavelet transform was proposed in [4]. The SAR echo is represented in time-frequency domain, and the wavelet transform is performed on the magnitude of the instantaneous-spectrum. The wavelet coefficients corresponding to WBI are filtered out. The iterative adaptive approach (IAA) and orthogonal subspace projection (OSP) were used in [5] to suppress the WBI. The shortcoming of these non-parametric methods is that the characteristics of WBI may not be fully exploited, leading to signal loss. Other methods are based on parametric models. A method for interference suppression in noise radar was proposed in [6]. The phase of the interference is locally approximated by a polynomial, the coefficients of which are estimated by using the product high-order ambiguity function (HAF). The performance of the method depends on the order of the polynomial, and the fitting error is the main problem. A tensor technique for simultaneous narrowband and wideband interference suppression was developed in [7]. This method achieves desirable performance in the environment of complex interference. Nevertheless, multiple view approximation of the single-channel SAR data is adopted in this method. The assumption that the interferences have approximately stable frequency bands in a synthetic aperture period is the basis of the method. Therefore, the method is not suitable to suppress the interferences with variable frequency bands.

In this paper, a WBI suppression method via instantaneous frequency (IF) estimation and intrinsic chirp component decomposition (ICCD) is proposed. The WBI-corrupted SAR echo is transformed into a 2-D time-frequency representation (TFR) by the short-time Fourier transform (STFT). Then, the IFs of the WBI components are estimated. Finally, the WBI is extracted by using the ICCD. The proposed method is applied to the real SAR data contaminated by the simulated WBIs. The experimental results verify the effectiveness of the proposed method.

The rest of this paper is organized as follows. In Section II, the signal models for the WBI and the WBI-corrupted SAR echo are introduced. In Section III, the proposed method is presented in detail. The experimental results are shown in Section IV. Finally, the conclusions are drawn in Section V.

2 Signal Model

Each SAR echo can be regarded as a time series. The WBI-corrupted SAR echo can be expressed as the superposition of useful echoes, noise and the WBI

$$x(n) = s(n) + r(n) + y(n),\ n = 0,1,\cdots,N-1 \qquad (1)$$

where $x(n)$, $s(n)$, $r(n)$ and $y(n)$ denote the SAR echo, the useful echo, the noise and the WBI, respectively. N

is the number of samples. The WBIs considered in this paper are chirp-modulated (CM) WBI [3], generalized sinusoidal-modulated (GSM) WBI and irregular frequency modulation (IFM) WBI. The CM WBI can be expressed as

$$y_{CM}(n)=\sum_{k=1}^{N_c}A_k(n)\exp\left(j\left(2\pi f_k n+\pi\mu_k n^2\right)\right) \tag{2}$$

where $A_k(n)$, f_k and μ_k denote the amplitude, frequency and chirp rate of the kth component, respectively. N_c represents the number of components. Then, the GSM WBI can be formulated as

$$\begin{aligned}y_{GSM}(n)=\sum_{k=1}^{N_c}A_k(n)\exp\Big(j\Big(&2\pi f_k n+\pi\mu_k n^2\\&+\alpha_k\sin\left(2\pi\overline{f}_k n+\overline{\varphi}_k\right)\Big)\Big)\end{aligned} \tag{3}$$

where $A_k(n)$, f_k, μ_k, α_k, $\overline{f}_k$ and $\overline{\varphi}_k$ denote the amplitude, frequency, chirp rate, modulation factor, modulation frequency and the initial modulation phase of the kth component, respectively. Next, the IFM WBI can be modeled as

$$y_{IFM}(n)=\sum_{k=1}^{N_c}A_k(n)\exp\left(j\tilde{\varphi}_k(n)\right) \tag{4}$$

where $A_k(n)$ and $\tilde{\varphi}_k(n)$ denote the amplitude and instantaneous phase of the kth component, respectively. $\tilde{\varphi}_k(t)$ is assumed to be a differentiable function of the time t and the derivative of the IF is assumed to be continuous in this paper.

3 Theory and Methodology

3.1 IF Estimation for the WBI

First, a WBI-contaminated SAR echo is transformed into a time-frequency representation (TFR) $W(n,k)$ by the STFT. n is the index of time bins, and k is the index of frequency bins. Then, the (generalized) Viterbi algorithm is used to obtain a smooth ridge path going through the points with relatively large amplitudes in the TFR [8]. Here are the details.

The IF estimation can be represented as

$$\begin{aligned}\overline{IF}(n)=\arg\min_{\eta(n)\in\boldsymbol{\eta}}\Bigg[&\sum_{n=n_1}^{n_2}f\left(W\left(n,\eta(n)\right)\right)\\&+\sum_{n=n_1}^{n_2-1}g\left(\eta(n),\eta(n+1)\right)\Bigg]\end{aligned} \tag{5}$$

where $f\left(W\left(n,\eta(n)\right)\right)$ and $g\left(\eta(n),\eta(n+1)\right)$ are penalty functions of the path $\eta(n)$ in the time interval $[n_1,n_2]$. $\boldsymbol{\eta}$ is the set of all possible paths between n_1 and n_2.

The TFR values at a time index n are sorted in non-increasing order:

$$\begin{aligned}&W(n,k_1)\ge W(n,k_2)\ge\cdots\ge W(n,k_m)\ge\cdots\ge W(n,k_M)\\&k_m\in I_f,\ m=1,2,\cdots,M\end{aligned} \tag{6}$$

where I_f is the index set of frequency bins, M is the number of elements in I_f. m is the index within the sorted sequence. The function $f(x)$ can be formulated as

$$f\left(W\left(n,k_m\right)\right)=m-1 \tag{7}$$

The smoothness of the path is related to the penalty function $g\left(\eta(n),\eta(n+1)\right)$. $g(x,y)$ can be formed as

$$g(x,y)=\begin{cases}0, & |x-y|\le\delta\\ \xi\left(|x-y|-\delta\right), & |x-y|>\delta\end{cases} \tag{8}$$

where δ is a threshold denoting the maximal allowable IF variation between two consecutive points, and ξ is the penalty factor controlling the level of penalty. In this paper, we let $\delta=2$ and $\xi=10$.

The on-line recursive approach based on the generalized Viterbi algorithm presented in [8] is used to solve (5) and obtain the IF estimates. Then, the regrouping approach presented in [9] is used to refine the IF estimates.

3.2 WBI Suppression with ICCD

ICCD is a method to decompose a multicomponent signal [9]. In this section, ICCD is utilized to extracted WBI.

A SAR echo corrupted by N_c WBI components can be formulated as

$$\begin{aligned}&s(t)=\sum_{m=1}^{N_c}\tilde{a}_m(t)\exp\left(j2\pi\textstyle\int_0^t IF_m(u)du\right)+z(t),\\&t=t_0,\cdots,t_{N-1}\end{aligned} \tag{9}$$

where N is the number of the samples, $z(t)$ is the sum of the useful echo and the noise, and $\tilde{a}_m(t)=a_m(t)e^{j\varphi_m}$ is the complex envelop of the mth component. $\tilde{a}_m(t)$ is assumed to be a band-limited signal, which can be expanded as

$$\tilde{a}_m(t)=\sum_{k=-K}^{K}c_k^{(m)}\exp\left(j2\pi k f_0 t\right) \tag{10}$$

where $c_{-K}^{(m)},c_{-K+1}^{(m)},\cdots,c_0^{(m)},\cdots,c_{K-1}^{(m)},c_K^{(m)}$ is the complex Fourier coefficients of the envelope; $f_0=f_s/(QN)$ is the base frequency, where Q is a positive integer, and f_s is the sampling frequency. Here, we let $Q=4$. The equation (9) can also be written as

$$\mathbf{s}=\boldsymbol{\Phi}\mathbf{c}+\mathbf{z} \tag{11}$$

where $\mathbf{s}=[s(t_0),\cdots,s(t_{N-1})]^{\mathrm{T}}$, $\mathbf{z}=[z(t_0),\cdots,z(t_{N-1})]^{\mathrm{T}}$, $\mathbf{c}=[\mathbf{c}_1^{\mathrm{T}},\cdots,\mathbf{c}_M^{\mathrm{T}}]^{\mathrm{T}}$ ($(\cdot)^{\mathrm{T}}$ denotes transposition) with $\mathbf{c}_m=[c_{-K}^{(m)},c_{-K+1}^{(m)},\cdots,c_0^{(m)},\cdots,c_{K-1}^{(m)},c_K^{(m)}]^{\mathrm{T}}$, $\boldsymbol{\Phi}=[\boldsymbol{\Phi}_1,\cdots,\boldsymbol{\Phi}_M]$, and the elements of $\boldsymbol{\Phi}_m$ is

$$(\mathbf{\Phi}_m)_{pq} = \exp\left(j2\pi(q-K-1)f_0 t_{p-1} + j\varphi_m t_{p-1}\right) \quad p=1,2,\cdots,N;\ q=1,2,\cdots,2K+1 \tag{12}$$

where $\varphi_m(t) = 2\pi\int_0^t IF_m(u)du$. In order to estimate the coefficients, the following optimization problem is considered:

$$\overline{\mathbf{c}} = \arg\min_{\mathbf{x}}\left(\|\mathbf{s}-\mathbf{\Phi}\mathbf{c}\|_2^2 + \lambda\|\mathbf{c}\|_2^2\right) \tag{13}$$

where $\|\cdot\|_2$ denote the l_2-norm, and λ is the regularization parameter. Here, we let $\lambda = 1$. The solution of (13) can be obtained as

$$\overline{\mathbf{c}} = \left(\mathbf{\Phi}^{\mathrm{H}}\mathbf{\Phi} + \lambda\mathbf{I}\right)^{-1}\mathbf{\Phi}^{\mathrm{H}}\mathbf{s} \tag{14}$$

Then, the *m*th WBI component can be reconstructed as

$$\overline{\mathbf{WBI}}_m = \mathbf{\Phi}_m\overline{\mathbf{c}}_m \tag{15}$$

where $\overline{\mathbf{c}}_m$ is the sub-vector corresponding to $\mathbf{c}_m$. The whole WBI is estimated as

$$\overline{\mathbf{WBI}} = \mathbf{\Phi}\overline{\mathbf{c}}. \tag{16}$$

The echo can be recovered by

$$\overline{\mathbf{z}} = \mathbf{s} - \overline{\mathbf{WBI}}. \tag{17}$$

4 Experimental Results

In this section, numerical experiments are carried out on the real SAR data with simulated WBIs. Here, we set $N_c = 4$. The ground-truth image is generated with the real SAR data. The amplitude of the WBI is adjusted and added to the original SAR data, and the signal-to-interference ratio (SIR) is -12dB. Here is an example. The TFR of a WBI-contaminated SAR echo is shown in Figure 1. In the experiment, the interference suppression approach based on the time-frequency transform and wavelet transform (TFTWT), the instantaneous-spectrum notch filtering (ISNF) and the eigensubspace projection (ESP) are used for performance comparison. The proposed method is denoted by ICCD.

In this paper, the recovery error (RE) of the SAR echoes is used to evaluate the performance of these methods quantitatively, which can be defined as

$$\mathrm{RE}(\mathbf{Z},\overline{\mathbf{Z}}) = 20\log_{10}\frac{\|\mathbf{Z}-\overline{\mathbf{Z}}\|_F}{\|\mathbf{Z}\|_F} \tag{18}$$

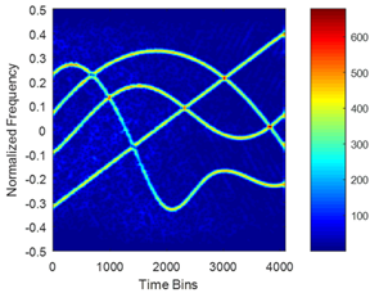

Figure 1. The TFR of a WBI-contaminated SAR echo.

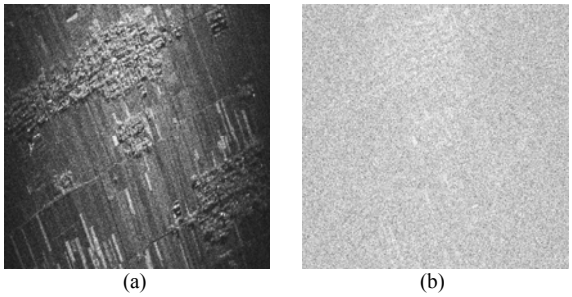

Figure 2. (a) Interference-free SAR image. (b) WBI-contaminated SAR images.

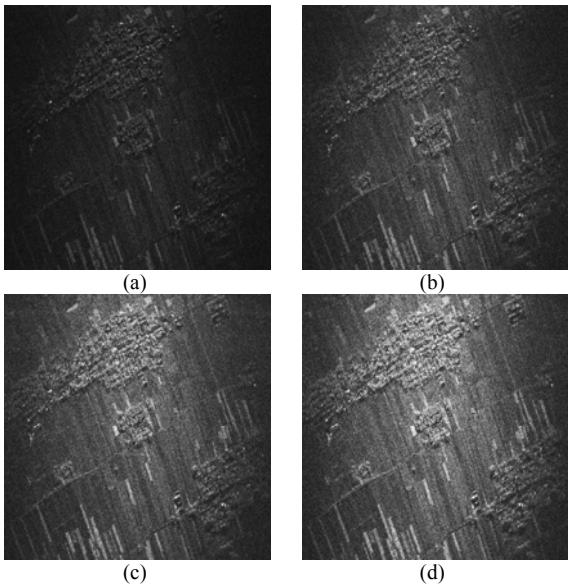

Figure 3. WBI suppression results. (a) TFTWT; (b) ISNF; (c) ESP; (d) ICCD.

Table 1. Performance comparison of different methods.

Method	TFTWT	ISNF	ESP	ICCD
RE (dB)	-2.75	-5.07	-6.85	-10.48
REI (dB)	-2.62	-4.59	-6.30	-10.07

where $\mathbf{Z}$ denotes the matrix containing interference-free SAR echoes as the columns, $\overline{\mathbf{Z}}$ is the matrix of the recovered echoes, and $\|\cdot\|_F$ is the Frobenius norm of a matrix. In order to evaluate the image quality, the recovery error of the SAR images can be defined as

$$\mathrm{REI}(\mathbf{G},\overline{\mathbf{G}}) = 20\log_{10}\frac{\|\mathbf{G}-\overline{\mathbf{G}}\|_F}{\|\mathbf{G}\|_F} \tag{19}$$

where $\mathbf{G}$ is the interference-free SAR image, and $\overline{\mathbf{G}}$ is the SAR image obtained with the recovered SAR echoes.

The interference-free SAR image and the WBI-contaminated SAR image (SIR= -12dB) are shown in Figure 2. The horizontal direction and the vertical direction represent azimuth and range, respectively.

The WBI suppression results of different methods are presented in Figure 3. There is a larger signal loss for TFTWT because the WBI and the useful echoes interfere with each other in the time-frequency plane, which makes it difficult to filter out the wavelet coefficients corresponding to WBI. ISNF relies on the frequency notches to mitigate WBIs in the instantaneous-spectrums, causing strong sidelobes in the time domain. The resulting image by using ESP is relatively dark, indicating the signal loss. The performance comparison of different methods is shown in Table 1. The proposed method achieves the best performance.

5 Conclusion

The existence of WBI severely affects the analysis of the radar echoes and the SAR image formation. In this paper, a method combining IF estimation and ICCD is proposed to suppress the WBI. First, the TFR of a WBI-contaminated SAR echo is obtained by using the STFT. Then, the IFs of WBI components are estimated by using the Viterbi algorithm and regrouping approach. Next, the ICCD is performed with the estimated IFs. The WBI components are extracted and the SAR echoes are recovered. Finally, the well-focused SAR image can be obtained. The experiments with the real SAR data and simulated WBIs demonstrate the effectiveness of the proposed method.

6 Acknowledgements

The authors would like to thank all anonymous reviewers for their useful comments and suggestions, which were of great help in improving this paper. This work was supported in part by the Fundamental Research Funds for the Central Universities under Grants XJS200204, XJS17070, NSIY031403 and 3102017jg02014; by the Natural Science Foundation of China under Grants 62001350, 61801347, 61801344, 61522114, 61471284, 61571349, 61631019, 61871459, 61801390 and 11871392; by the China Postdoctoral Science Foundation under Grants 2020M673346, 2017M613076 and 2016M602775; by the NSAF under Grant U1430123; by the Natural Science Basic Research Plan in Shaanxi Province of China under Grant 2018JM6051; by the Aeronautical Science Foundation of China under Grant 20181081003; by the Science, Technology and Innovation Commission of Shenzhen Municipality under Grant JCYJ20170306154716846; and by the Innovation Fund of Xidian University.

7 References

1. B. Zhao, L. Huang, J. Li and P. Zhang, “Target Reconstruction From Deceptively Jammed Single-Channel SAR,” *IEEE Trans. Geosci. Remote Sens.*, **56**, 1, Jan. 2018, pp. 152-167, doi: 10.1109/TGRS.2017.2744178.

2. Y. Huang, G. Liao, J. Xu and J. Li, “GMTI and Parameter Estimation via Time-Doppler Chirp-Varying Approach for Single-Channel Airborne SAR System,” *IEEE Trans. Geosci. Remote Sens.*, **55**, 8, Aug. 2017, pp. 4367-4383, doi: 10.1109/TGRS.2017.2691742.

3. M. Tao, F. Zhou and Z. Zhang, “Wideband Interference Mitigation in High-Resolution Airborne Synthetic Aperture Radar Data,” *IEEE Trans. Geosci. Remote Sens.*, **54**, 1, Jan. 2016, pp. 74-87, doi: 10.1109/TGRS.2015.2450754.

4. S. Zhang, M. Xing, R. Guo, L. Zhang and Z. Bao, “Interference Suppression Algorithm for SAR Based on Time-Frequency Transform,” *IEEE Trans. Geosci. Remote Sens.*, **49**, 10, Oct. 2011, pp. 3765-3779, doi: 10.1109/TGRS.2011.2164409.

5. Z. Yang, W. Du, Z. Liu and G. Liao, “WBI Suppression for SAR Using Iterative Adaptive Method,” *IEEE J. Sel. Topics Appl. Earth Observ. Remote Sens.*, **9**, 3, Mar. 2016, pp. 1008-1014, doi: 10.1109/JSTARS.2015.2470107.

6. S. Djukanovic and V. Popovic, “A Parametric Method for Multicomponent Interference Suppression in Noise Radars,” *IEEE Trans. Aerosp. Electron. Syst.*, **48**, 3, Jul. 2012, pp. 2730-2738, doi: 10.1109/TAES.2012.6237624.

7. Y. Huang, L. Zhang, J. Li, W. Hong and A. Nehorai, “A Novel Tensor Technique for Simultaneous Narrowband and Wideband Interference Suppression on Single-Channel SAR System,” *IEEE Trans. Geosci. Remote Sens.*, **57**, 12, Dec. 2019, pp. 9575-9588, doi: 10.1109/TGRS.2019.2927764.

8. I. Djurovi´c and L. Stankovi´c, “An Algorithm for the Wigner Distribution Based Instantaneous Frequency Estimation in A High Noise Environment,” *Signal Process.*, **84**, 3, Mar. 2004, pp. 631-643, doi:10.1016/j.sigpro.2003.12.006.

9. S. Chen, X. Dong, G. Xing, Z. Peng, W. Zhang and G. Meng, “Separation of Overlapped Non-Stationary Signals by Ridge Path Regrouping and Intrinsic Chirp Component Decomposition,” *IEEE Sensors J.*, **17**, 18, Sept.2017, pp. 5994-6005, doi: 10.1109/JSEN.2017.2737467.